01

Relative orientation dynamics of stabilized CH_3 radicals and matrix CH_4 molecules in solid methane in 1.4−35 K temperature region

© Yu.A. Dmitriev

Ioffe Institute, St. Petersburg, Russia

e-mail: dmitriev.mares@mail.ioffe.ru

Received April 28, 2025
Revised June 03, 2025
Accepted October 24, 2025

Results are presented on CH_3 radical stabilization in solid CH_4 matrix from the gas phase and their study by EPR. In the first series of experiments, the samples are obtained by deposition on a substrate at $T_{dep} = 4.2$ K and studied in temperature range $T_{rec} = 1.4-4.2$ K. In the second series of the experiments, the relevant temperatures are: $T_{dep} = 15-17$ K, $T_{dep} = 15-17$ K. The relative intensity of the forbidden electron-proton transitions is measured versus microwave power and the sample temperature. The experimental result analysis testify to existence of two temperature regions with different degrees of correlation between the radical and matrix molecules orientation motion.

Keywords: electron paramagnetic resonance, matrix isolation, methyl radical, solid methane, molecular rotation.

DOI: 10.61011/EOS.2025.10.62550.7915-25

Methyl radicals CH_3 stabilized in a solid methane CH_4 matrix, represent a „quantum rotator in a matrix of quantum rotators“ even at sample temperatures significantly higher than helium ones. This follows from the smallness of the rotational constant, $B = 6.76$ K for rotation around the third-order axis C_3 of the free molecule, which results in an energy spacing between the lowest rotational states of about 20 K. To describe a quantum rotator in liquid and solid media of quantum particles, a model of a new quasiparticle—the angulon—has recently been proposed [1] and is actively being developed [2,3]; it represents the impurity molecule as a particle—rotator in a „coat“ of phonons or other multi-particle excited states of the matrix medium that possess angular momentum [3]. Until now, the only experiments on which this model is based are those involving the trapping of molecules in nanodroplets of superfluid helium. In solid methane, multi-particle excited states can, in particular, be played by quasiparticles called topons — collective orientational motions of molecules, the existence of which was proposed to describe the features of the temperature dependence of the specific heat capacity of solid CH_4 [4] and has found indirect confirmation in the features of the orientational motion of CH_3 in a CD_4 matrix [5].

Among the applied significances of the CH_3/CH_4 system, one can highlight its role in chemical processes occurring in cold clouds in interstellar space, on the surfaces of comets, and in the atmospheres of Solar System planets and their satellites. The starting stage for the subsequent chain of low-temperature chemical reactions in solid methane yielding heavy hydrocarbons is the photolysis of methane [6]:

$$CH_4 + h\nu \rightarrow CH_3 + H.$$

Ethane, which is the second most abundant hydrocarbon in planetary atmospheres and cosmic space after CH_4 is efficiently formed at low temperatures in the reaction $2CH_3 \rightarrow C_2H_6$. We also note the role of solid methane as a promising cold neutron moderator, whose radiation resistance under a neutron beam is limited by the formation of a certain amount of radiolytic hydrogen and „frozen“ radicals, including methyl ones [7].

In this work, EPR studies have advanced the investigation of the correlation, previously discovered, between the orientational motion of the methyl radical stabilized in the temperature range $1.4 - 4.2$ K and the orientational motion of the matrix molecules CH_4 (CD_4) [8,9]. The relative intensity of forbidden electron-nuclear transitions of radicals, measured at helium temperatures [8], suggests a certain preferential orientation of neighboring CH_4 molecules relative to the impurity CH_3 molecule in the *A*-symmetric state, which persists in the dynamics of their mutual orientational motion.

In Fig. 1, *a*, *b* the experimental EPR spectra of the CH_3 radical stabilized in a solid CH_4 matrix by vapor-phase deposition are presented, recorded at sample temperatures of 1.73 and 29.9 K, respectively. The first of these spectra was obtained in a series of low-temperature experiments with deposition onto a substrate at 4.2 K located at the center of an evacuated microwave cavity of a mixture of gaseous methane supplied through the matrix channel and products of a high-frequency gas discharge in methane from a separate discharge tube. The second spectrum (Fig. 1, *b*) was obtained in a series of high-temperature experiments in which a mixture of CH_4:He (2:25) was passed through the discharge, while pure methane was supplied through the matrix channel. Deposition occurred onto a substrate at $T_{dep} = 15-17$ K. The EPR spectrum of the CH_3 radical

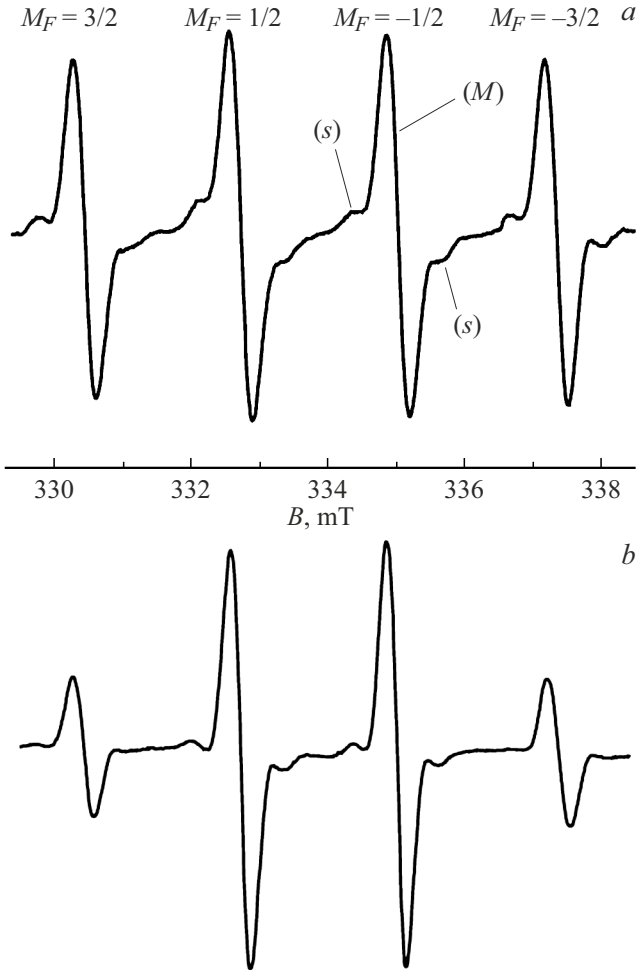

Figure 1. EPR spectrum of the CH_3 radical stabilized in a solid CH_4 matrix. (a) The low-temperature sample was obtained by deposition from the gas phase onto a substrate at $T_{dep} = 4.2$ K. The experimental spectrum was recorded at a temperature of $T_{rec} = 1.73$ K and an electromagnetic wave power incident on the microwave resonator of 0.15 μW. The spectrometer resonance frequency is $f_{res} = 9359.20$ MHz. Here s — forbidden transitions appearing as satellites of the allowed transition M. (b) The high-temperature sample was obtained and studied under the following experimental parameters: $T_{dep} = 15-17$ K, $T_{rec} = 29.9$ K, microwave power 0.15 μW. For convenience of comparison, the position of the high-temperature spectrum in the magnetic field has been recalculated to the resonance frequency of 9359.20 MHz.

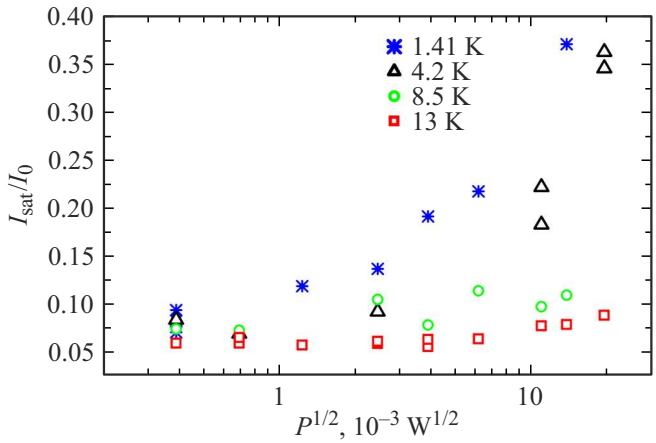

Figure 2. Dependence of the relative intensity of satellite lines of the low-field and high-field hyperfine components of the CH_3 EPR spectrum in CH_4 on the microwave power in the spectrometer resonator for samples at various temperatures. Here I_{sat} — intensity of the satellite, I_0 — intensity of the allowed line. Results denoted by blue stars correspond to a sample temperature of 1.41,K, black triangles — 4.2 K, green circles — 8.5 K, red squares — 13 K. The maximum and minimum values of the square root of the microwave power plotted on the abscissa axis were obtained at powers of 0.15 and 377 μW respectively.

contains four intense lines and represents an unresolved superposition of a quartet and a doublet of hyperfine components, which are the first derivatives of absorption lines. Symmetric nuclear spin A-states (total nuclear spin equal to 3/2) give a hyperfine quartet in the EPR spectrum, while antisymmetric E-states (total nuclear spin equal to 1/2) give a doublet. The positions of the doublet lines in the magnetic field nearly coincide with the positions of the two central lines of the quartet, which, given a linewidth of about 0.35 mT, results in these two multiplets not being resolved in the spectrum. In Fig. 1, a the designation (M) corresponds to allowed transitions, while (s) denotes weak resonant satellite lines associated with forbidden electron-nuclear transitions involving simultaneous flipping of the spin of the unpaired electron and the spin of the nucleus of a neighboring matrix molecule. The preferential population at low temperatures of the ground rotational state, which is A-symmetric, is reflected in the ratio of amplitudes and intensities of the allowed hyperfine components close to 1:1:1:1. At high temperatures, not only the ground state but also the first excited E-symmetric state, as well as subsequent excited rotational states, are populated. This leads (Fig. 1, b) to the characteristic high-temperature intensity ratio of 1:3:3:1.

The relative intensity of satellites is determined as I_{sat}/I_0, where I_{sat} — intensity of the satellite I_0 — intensity of the allowed line. The relative intensity of the satellite provides information on the number of nearest matrix molecules and their distance [10], as well as on the preferential mutual orientation of the radical and matrix molecules [8]. At helium temperatures, a significant factor complicating spectrum analysis is the much stronger saturation of allowed lines compared to forbidden resonances upon increasing the microwave power in the resonator. This can lead to distortion of the relative contribution of satellites, which should thus be determined from spectra at low microwave power levels. Fig. 2 shows the ratios I_{sat}/I_0 measured from the spectra as a function of the square root of the microwave power in the resonant cavity at various temperatures. From the figure, it follows that the function $I_{sat}/I_0(P^{1/2})$ is highly sensitive to temperature and already at $T_{rec} = 8.5$ K is close to a constant. The estimated maximum microwave

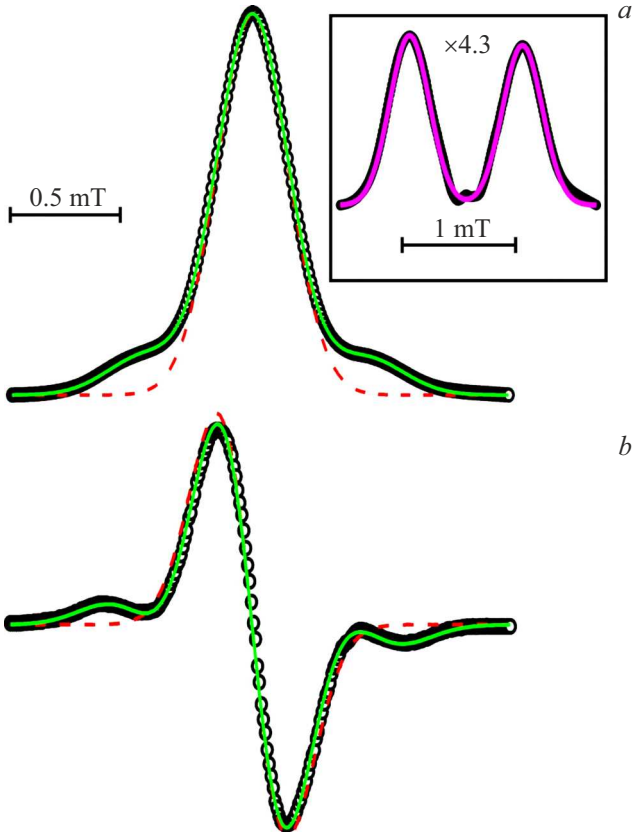

Figure 3. Modeling of the high-field, $M_F = -3/2$, hyperfine component of the CH_3 radical EPR spectrum. The spectrum was obtained at a sample temperature of $T_{rec} = 8.5$ K and microwave power in the resonant cavity of 189 μW. (a) Modeling of the absorption line. Here black circles — resonance curve obtained by integrating the experimental spectrum; red dashed curve — calculated Gaussian curve modeling the main (allowed) EPR line; green solid curve — modeling of the experimental result by superposition of the main and satellite lines. The inset shows, at 4.3 magnification, the difference curve of the experimental (black circles) and calculated (red dashed curve) resonances, representing the satellite spectrum. Modeling of this difference curve is shown by the purple line and calculated as a superposition of two Gaussian resonance curves. (b) Modeling of the first derivative of absorption. Here black circles — experimental result; red dashed curve — calculated Gaussian curve modeling the main (allowed) EPR line; green solid curve — modeling of the experimental result by superposition of the main and satellite lines.

power values for measuring intensity ratios are as follows: 0.15 μW (1.41 K), 1 μW (4.2 K), 9 μW (8.5 K), 49 μW (13 K). This result agrees with the corresponding value of 10 μW reported in [10] for a CH_3 sample in CH_4 at 10 K.

The experimental spectrum was processed as follows (Fig. 3). By integrating the experimental curve (black circles, Fig. 3, b) of the hyperfine component, in this case $M_F = -3/2$, we obtained the resonance absorption line— black circles in Fig. 3, a. The allowed absorption line was modeled by a Gaussian curve (red dashed curve in Fig. 3, a) and its derivative (red dashed curve in Fig. 3, b). The

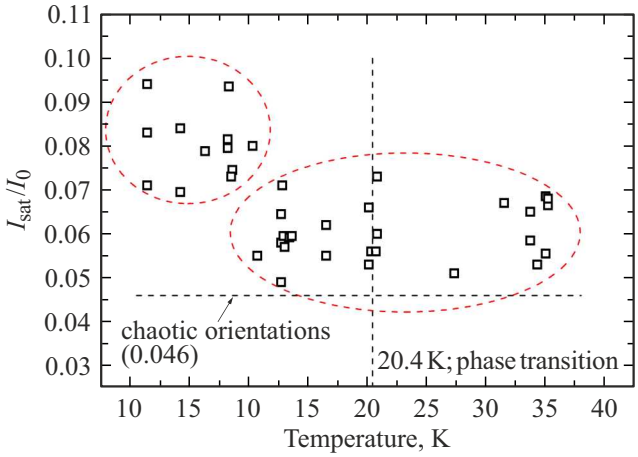

Figure 4. Dependence of the relative intensity of satellite lines of the low-field and high-field hyperfine components of the CH_3 EPR spectrum in CH_4 on the sample temperature.

satellite spectrum was isolated as the difference between the experimental and calculated (Gaussian) curves black circles in the inset of Fig. 3, a. The satellites were modeled as a superposition of two Gaussian lines — purple solid curve. The superpositions of allowed and forbidden resonances (solid green lines in Fig. 3, a, b) reproduce the experiment well.

The obtained results for the relative intensity of satellites as a function of sample temperature are shown in Fig. 4. The considerable scatter of points on the graph is explained by the fact that the satellites have low intensity and are isolated as the result of subtracting two quantities of significantly greater intensity: the experimental and calculated ones. From the figure, it is evident that the set of experimental values splits into two groups: low-temperature and high-temperature. The dashed line parallel to the abscissa axis corresponds to the contribution of satellites to the resonance line intensities for chaotic orientation of matrix molecules neighboring the stabilized radical [8]. The vertical dashed line corresponds to the temperature (20.4 K) of the transition in solid methane from the low-temperature phase II with partial orientational ordering of CH_4 molecules to the high-temperature phase I without orientational order. The various orientational phases of solid CH_4 and transitions between them were identified from calorimetric studies, coherent neutron scattering, X-ray scattering, time-of-flight pulsed powder neutronography, thermal conductivity studies, and others. Phase II is characterized by the presence of eight sublattices, in two of which the molecular field vanishes and the CH_4 molecules are thus unoriented. Six out of eight methane molecules are orientationally ordered. The crystal structure corresponding to the centers of mass of the molecules is face-centered cubic. The low-temperature phase III, corresponding to complete orientational ordering of the molecules, was observed at zero pressure only for heavy methane CD_4 at temperatures below 22.1 K. In turn, the phase transition

I–II in CD_4 occurs at 27.0 K. Previously, in experiments on stabilizing CH_3 in CD_4 [9] it was found that methyl radicals trapped in the low-temperature matrix (phase III) change symmetry from the planar D_3 characteristic of the free molecule to pyramidal C_3. With increasing sample temperature and transitions of the matrix orientational structure to phases II and I, a noticeable fraction of molecules about 40% in the first case and 50% in the second restores the planar structure. These results were obtained by studying the temperature dependence of the relative intensity of the allowed doublet and quartet lines, which changes depending on the population of the rotational levels of the CH_3 radical. The dramatic decrease in the rotational constant for CH_3 in CD_4, $B = 3.15$ K, as compared to the value for the free molecule $B_{\text{free}} = 6.76$ K, should also be noted. The same change in the rotational constant was observed in experiments at helium temperatures on stabilizing CH_3 in CH_4 [11]. From Fig. 4, it follows that the transition at 20.4 K from phase I of solid CH_4 to phase II does not noticeably affect the mutual orientation of the radical and matrix molecules. This conclusion correlates with the result described above regarding the small change in the symmetry of CH_3 molecules in CD_4 upon the phase I – phase II transition. As for the abrupt change in the relative intensity of satellites (Fig. 4), the approximate temperature of this change, $T_{\text{trans}} = 10$ K, is nearly equal to the temperature of the transition of the linear expansion coefficient of solid CH_4 from positive to negative values [12,13]. Thus, the crystal cell volume reaches a minimum and is followed by expansion with changing temperature. The negative linear expansion coefficient is a characteristic feature specifically of light solid methane CH_4 and is not observed in heavy CD_4. Methane CH_4 is a mixture of three spin modifications A, T, E with total nuclear spin of the molecules 2, 1, 0, respectively. The ground rotational state ($J = 0$) has A-symmetry and corresponds to the lowest energy of the molecule. While the time of conversion to the CH_4 low-energy states takes several hours after sample deposition of pure methane [14], this time reduces to seconds for molecules near a paramagnetic impurity, e. g., the CH_3 radical. Each CH_4 molecule in solid methane is in a crystal field with several equivalent minima between which it can tunnel, leading to tunnel splitting of the rotational levels. For a low barrier height, the level splitting in energy is large, and as the height increases, the tunneling probability decreases, and thus the level splitting decreases. The equilibrium cell volume at a given temperature corresponds to the minimum of the free energy as a function of volume. Contributions to the free energy are made by [12,13] tunnel levels, whose population changes with temperature, elastic deformation, and lattice excitations associated with librons and phonons. At low temperatures, the first two components predominate, determining the essentially quantum character of the linear expansion coefficient and its negative value in this range. At high temperatures, the third component dominates, leading to a positive coefficient and its classical temperature dependence. Thus, the boundary observed in our experiment at $T_{\text{trans}} \sim 10$ K between two preferential mutual orientations of the CH_3 radical and neighboring CH_4 molecules corresponds to the transition between the ranges of predominantly quantum and predominantly classical nature of the free energy of solid methane.

Conflict of interest

The author declares that he has no conflict of interest.

References

[1] R. Schmidt., M. Lemeshko. Phys. Rev. Lett., **114** (20), 203001 (2015). DOI: 10.1103/PhysRevLett.114.203001
[2] Y.Y. Liu, Y. Cui, X.Z. Shang, R.B. Yang, Z.Q. Li, Z.W. Wang. J. Chem. Phys., **159**, 114305 (2023). DOI: 10.1063/5.0162004
[3] Z. Zeng, E. Yakaboylu, M. Lemeshko, T. Shi, R. Schmidt. J. Chem. Phys., **158**, 134301 (2023). DOI: 10.1063/5.0135893
[4] A.Yu. Zaharov, A.V. Leont'eva, A.Yu. Prohorov, A.I. Erenburg. FTT, **56** (7), 1446 (2014) (in Russian). https://journals.ioffe.ru/articles
[5] A.Yu. Prokhorov, A.V. Leont'eva, Yu.A. Dmitriev. J. Phys: Conf. Ser., **1352**, 012041 (2019). DOI: 10.1088/1742-6596/1352/1/012041
[6] B. Gans, S. Boyé-Péronne, M. Broquier, M. Delsaut, S. Douin, C.E. Fellows, P. Halvick, J.-C. Loison, R.R. Lucchese, D. Gauyacq. Phys. Chem. Chem. Phys., **13**, 8140 (2011). DOI: 10.1039/C0CP02627A
[7] O. Kirichek, C.R. Lawson, D.M. Jenkins, C.J.T. Ridley, D.J. Haynes. Cryogenics, **88**, 101 (2017). DOI: 10.1016/j.cryogenics.2017.10.017
[8] Yu.A. Dmitriev. Opt. i spektr., **132** (11), 1108 (2024) (in Russian). DOI: 10.61011/OS.2024.11.59491.6359-24
[9] Yu.A. Dmitriev, N.P. Benetis. J. Phys. Chem. A., **122**, 9483 (2018). DOI: 10.1021/acs.jpca.8b09478
[10] F.J. Adrian, B.F. Kim, J. Bohandy. J. Chem. Phys., **82** (4), 1804 (1985). DOI: 10.1063/1.448414
[11] Yu.A. Dmitriev. Opt. i spektr., **129** (9), 1129 (2021) (in Russian). DOI: 10.21883/OS.2021.09.51337.2140-21
[12] Yu.A. Freiman, V.V. Vengerovsky, A.F. Goncharov, Fiz. Nizk. Temp., **46** (2), 219 (2020). DOI: 10.1063/10.0000537
[13] Yu.A. Frejman. FNT, **9** (6), 657 (1983) (in Russian).
[14] A.N. Aleksandrovskij, V.B. Kokshenyov, V.G. Manzhelij, A.M. Tolkachyov, FNT, **4** (7), 915 (1978). (in Russian)

Translated by J.Savelyeva